THORIUM(IV) SORPTION ONTO SODIUM BENTONITE AND MAGNETIC BENTONITE

Abdelkader Miraoui[a] and Mohamed Amine Didi[a]*

Keywords: Bentonite; nanoparticle; isotherm; thorium; magnetic process.

In this paper, the liquid-solid extraction of thorium(IV) by sodium bentonite and magnetic bentonite is reported. Magnetic adsorbent can be quickly separated from a medium by a simple magnetic process. Various parameters have been studied to assess the performance of maghemite nanocomposite clay for the removal of Th(IV). The operating variables studied are initial Th(IV) concentration, pH, ionic strength, temperature and contact time. The time needed for magnetic bentonite to adsorb the maximum of Th(IV) is 45 min and 60 min for sodium bentonite. For magnetic bentonite, optimal extraction yield was achieved at an initial pH equal at 6.2 and for sodium bentonite, the variation of initial pH has no influence on the extraction yield. The sorption capacities of sodium bentonite and magnetic bentonite are 41.24 and 31.34 $mg.g^{-1}$ respectively. Adsorption equilibrium data were calculated for Langmuir and Freundlich isotherms. It was found that the sorption of Th(IV) on sodium and magnetic bentonite was better suited to the Langmuir adsorption model. Thermodynamics data leads to endothermic and spontaneous process for magnetic bentonite and exothermal for sodium bentonite. The quantitative elution study of thorium can be realized with acetic acid for sodium bentonite and sulfuric acid for magnetic bentonite.

* Corresponding Authors
Fax: +21343213198
E-Mail: madidi13@yahoo.fr
Laboratory of Separation and Purification Technologies,
Department of Chemistry- Faculty of Sciences, Box119.
Tlemcen University -13000, Algeria.

Introduction

Industrial activities generate a wide diversity of wastewaters, often containing agents that cause pollution, which can cause dangerous consequences for human beings by affecting the ecosystems.[1] Due to the high toxicity of radioactive metals, exposure to these pollutants is a problem for human health and contamination of the environment, hence removal of these heavy metals from eco-system is necessary.[2,3] Significant research efforts are currently directed towards removing radioactive ions such as thorium, uranium and other actinides from residual waters.[4] Thorium is abundantly available in earth's crust in association with rare earths and uranium,[5] it is about three times more abundant than uranium.[6] Thorium is only stable at its four valence state in solution.[7] The main sources of thorium are monazite, rutile and thorianite. It occurs in the tetravalent form in its compounds in nature,[8] the major sources of it in nature are plants, sand, soil, rocks and water. Normally, very little amounts of thorium from rivers, oceans, and lakes are accumulated into fish or seafood.[9-11] Since the last century, thorium has been extensively used in a variety of applications in various fields like geology, metallurgy, chemical industry, nuclear industry and medicine.[5,12,13] Thorium oxide finds application as catalyst, high temperature ceramic and high quality lenses.[11]

In view of the extensive use of radioactive elements in various industries, their leakage, even at trace levels, has been a public health problem for many years and causes serious environmental hazards,[1,11,14,15] for example, these elements affect the human health by changes in genetic material of body cell and causing diseases like the lung and liver cancers.[9,15,16]

To safeguard human life, cost-effective removal of thorium from eco-system has received much attention.[17] The most widely used techniques for separation of thorium include liquid-liquid extraction, ion exchange, chemical precipitation, extraction chromatography, membrane dialysis, flotation, electrodeposition and adsorption.[5,10,14] Sorption and ion exchange are the most popular methods for the removal of toxic or radioactive metal ions from aqueous solution. High efficiency, simple operation and environmental compatibility are some of the advantages of sorption process.[14,16] Various types of materials have been used for thorium sorption, for example activated carbon,[18] modified clays,[19] XAD-4 resin,[20] hematite,[21] PAN/Zeolite.[22] However, because of its relatively high cost, there have been attempts to utilize low cost and efficient, locally available materials for the removal of thorium.[23] In recent years, the preparation of organic–inorganic superabsorbent composites has attracted great attention because of their relatively low production cost, high water absorbency and their considerable range of applications in agriculture and horticulture.[24] Recently, clays and clay minerals were found to be very important for preparation of this superabsorbent nanocomposite.[25] In this regard, montmorillonite-rich materials like bentonites exhibit highly interesting properties, e.g. high specific surface area, cation exchange capacity (CEC), porosity, and tendency to retain water or other polar and non-polar compounds.[26] The clay used in this work is bentonite because of its natural abundance and low cost,[24] it is found in many places of the world. Any clay of volcanic origin that contains montmorillonites is referred to as bentonite. Bentonite belongs to the 2:1 clay family, the basic structural unit of which is composed of two tetrahedrally coordinated sheets of silicon ions surrounding a octahedrally coordinated sheet of aluminium ions. Compared with other clay types, bentonite has excellent adsorption properties and possesses adsorption sites available within its interlayer space as well as on the outer surface and edges. Therefore, bentonite has recently been employed in many separation applications with or without modification.[27] Removal by clay is a simple and low cost technology. However, some problems

still exist with regard to the application of clay technique like, unacceptable low adsorption capacity and difficulty in the separation of the resulting solid waste. Magnetic adsorbent can be quickly separated from a medium by a simple magnetic process, in view of this property, we have studied a new strategy toward multifunctional magnetic bentonite material.[28] The objectives of this study are to assess the performance of maghemite nanocomposite clay for the removal of thorium ions. Effects of pH and temperature on the adsorption process are also investigated. used to determine the best isotherm equation which represents the experimental Further studies can explore the possible regeneration of nanocomposite clay for reuse.[31]

Experimental

Reagents

Thorium solution at 10^{-2} M was prepared by dissolving of $Th(NO_3)_4$. 4 H_20 (from FLUKA) (0.552 g) in 100 mL of distilled water. The initial pH of the sample solutions were adjusted by using dilutes HNO_3 or NaOH (from Sigma-Aldrich). $NaNO_3$, sodium acetate and NaS_2O_3 (from Merck) were used in the salt effect. Arsenazo III 10^{-3} M (from Fluka) was prepared by dissolving 0.0820 g in absolute ethanol. Hydrochloric acid (from Organics), sulfuric acid (from Fluka), nitric acid (from Cheminova), and acetic acid (from Riedel Dehaen) were used from elution study.

The natural bentonite used in this study was obtained from deposits in the area of Maghnia, Algeria.

For synthesis of magnetic nanoparticles, $FeCl_2.4H_2O$ (from Sigma-Aldrich), $FeCl_3.6H_2O$ (from Panreac), NH_4OH (from Sigma-Aldrich), HNO_3 and $Fe(NO_3)_2$ (from Sigma-Aldrich) were used.

Apparatus

The extraction of Th(IV) was studied by the batch process using a stirring vibrator (Haier model). pH measurements were performed with a pH meter using a combined electrode mark (Adwa). Thermogravimetric analyses of samples (TGA) were performed using a SDT Q600 thermogravimetric analyzer at a heating rate of 20 °C/min under nitrogen atmosphere, Tlemcen–Algeria. The BET-N_2 method was used to determine the specific surface area of the bleaching earths, using a Volumetric Analyzer (Nova-1000). A magnet and centrifugation for the recovery of the magnetic particles and sodium bentonite, respectively, in the aqueous phase were used. Samples containing Th(IV) were analyzed by spectrophotometer (Analytik Jena Specord 210 Plus, at Tlemcen-Algeria) with Arsenazo III as ligand.

Preparation of sodium bentonite

For the purification of bentonite, 120 g of natural bentonite was dispersed in 1.5 L of distilled water, and after agitation during 15 min, a buffer solution of sodium citrate (pH 7.3) was added. The mixture was heated under agitation at 75° C for 20 min and then, 15 g of sodium thiosulfate ($Na_2S_2O_4$) was slowly added. After 15 min under agitation, the mixture was cooled and centrifuged at a rotational speed of 6000 rpm for 15 min. The solid recovered was washed two times with HCl 0.05 M (1.5 L) during 3 h.

To convert the purified bentonite into sodium form an amount of bentonite was dispersed in NaCl solution (1 M) with a 1/5 mass ratio and after agitation for 2 h, the solid was separated by centrifugation at a rotational speed of 6000 rpm for 15 min, this operation was repeated three times. The solid was washed three times with distilled water, and it was dried at 40° C for 3 days.

The chemical composition of purified bentonite was found to be 64.7 % SiO_2, 18.1 % Al_2O_3, 0.95 % Fe_2O_3, 2.66 % MgO, 0.8 % K_2O, 0.61 % CaO, 0.2 % TiO_2, 1.43 % Na_2O, 0.05% As, 10.0% loss on ignition. The cation-exchange capacity (CEC) of bentonite was determined according to the ammonium acetate saturation method and was found to be 70 mEq per 100 g of dry natural-Bt and 98 mEq per 100 g of dry Na–Bt. The BET specific surface area increase from 50 m^2 g^{-1} in natural-Bt to 95 m^2 g^{-1} in Na–Bt .[23]

Preparation of magnetic particles

The ferrofluid magnetic used was the maghemite (γ-Fe_2O_3) nanoparticles dispersed in an aqueous solution. Particles were synthesized by co-precipitation of a stoichiometric mixture of ferrous and ferric chloride in an ammonium hydroxide solution. The precipitate magnetite (Fe_3O_4) obtained was acidified by nitric acid (2 M) and oxidized into maghemite (γ -Fe_2O_3) at 90 °C with iron (III) nitrate. The maghemite particles obtained were precipitated by acetone, then dispersed into water leading to an ionic ferrofluid acid (pH=2.0). After these step, nanoparticles were positively charged, with nitrate as counter ions.[29,30]

Preparation of magnetic bentonite

The composites were prepared by dissolving $FeCl_3$ (7.8 g, 28 mmol) and $FeSO_4$ (3.9 g, 14 mmol) in 400 mL of water at 70 °C. 3.3, 6.6 or 9.9 g of clay bentonite was added in order to obtain the following adsorbent: iron oxide weight ratios 1.0:1.0, 1.5:1.0 and 2.0:1.0, respectively. To these suspensions was added a solution of NaOH (100 mL, 5 mol L^{-1}) drop wise to precipitate the iron oxides. The obtained solid materials was washed with distilled water and dried in an oven at 100 °C for 2 h. A simple test with a magnet (0.3 T) of the product showed that the whole material is completely attracted to the magnet.[32] Positive ferrous and ferric ions are co-precipitated on Bentonite due to the reactions between ferrous and ferric ions and silanol groups and aluminol groups of Bentonite.

$$Fe^{2+} + 2\ Fe^{3+} + 8\ OH^- + \text{Bentonite} \rightarrow \text{Bentonite-}Fe_3O_4 + 4H_2O \quad (1)$$

$$2\ Fe^{3+} + 5\ OH^- + \text{Bentonite} \rightarrow \text{Bentonite-}Fe_2O_3 + 2\ H_2O + H^+ \quad (2)$$

The BET specific surface area increases from 50 m^2 g^{-1} in sodium-Bt to 72 m^2 g^{-1} in magnetic–Bt.

Extraction and analysis procedure

The method of extraction used for this study, was carried out by a mixture of 4 mL of Th(IV) solution of known concentration, and 0.01 g of ther solid adsorbent (sodium bentonite and magnetic bentonite) in an Erlenmeyer with stopper, under vigorous stirring. Both liquid and solid phases were separated by centrifugation for sodium bentonite and magnet for magnetic bentonite, the solid phase was regenerated for other applications and the liquid phase was measured by the UV-visible spectrometer. The sample of Th(IV) was analyzed by a mixture of 100 µL ArsenazoIII and 100 µL of Th(IV) in a medium of 9 M HCl (2 mL). The product of interaction of Arsenazo III with Th(IV) was determined at λ_{max}= 660 nm.[33]

The percentage of thorium ions that was extracted by solids extractant was determined as by Eqn. 3.

$$E\,(\%) = 100\frac{C_i - C_e}{C_i} \qquad (3)$$

The amount of thorium uptakes at time *t*, q_t (mg g^{-1}), was calculated by Eqn. 4.

$$q_t\,(mg\ g^{-1}) = V * M * \frac{c_i - c_t}{w} \qquad (4)$$

where

C_i, C_t and C_e are the initial, time *t* and equilibrium Th(IV) concentration (mol L^{-1}), respectively,
V (4 mL) is the volume of the solution,
M molecular weight, and
w is the mass of the solids adsorbents (0.01 g).

Desorption procedure

After saturation of sodium bentonite and magnetic bentonite by the thorium ions, it can be regenerated for another extraction, using the following acids: HCl, HNO_3, H_2SO_4 and CH_3COOH. We can determine the best eluting with help of Eqn.5.

$$\text{Elution yield}\,(\%) = 100\,\frac{C_{elution}}{C_i - C_e} \qquad (5)$$

where

$C_{elution}$, concentration of Th(IV) (mol L^{-1}) after acid treatment.

Results and Discussion

Effect of contact time

To study this effect we obtained the extraction yields at different time (Fig. 1). It is seen that the extraction efficiency increases rapidly with increasing time. The time needed for magnetic bentonite to adsorb the maximum of Th(IV) is 45 min (58 %, 8.26 mg.g^{-1}) and 60 min for sodium bentonite (89 %, 8.65 mg.g^{-1}). Thus extraction with magnetic bentonite is more efficient than with sodium bentonite. The thorium does not occupy only the non-occupied spaces by the maghemite.

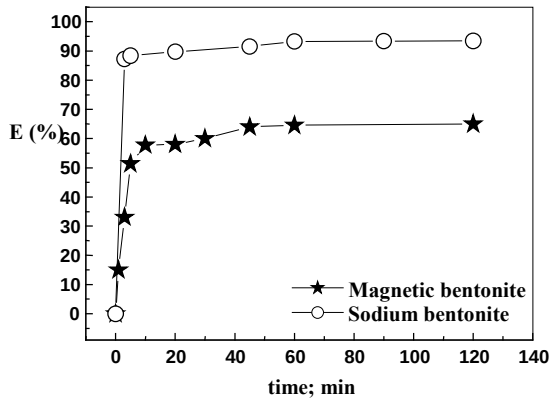

Figure 1. Removal of thorium by magnetic and sodium bentonites as a function of time. $[Th(IV)]_0$ = 1 x 10^{-4} mol L^{-1}, *w* = 0.01 g, *V* = 4 mL, Ø = 250 rpm, *T*= room temperature.

Adsorption kinetics

Kinetics of sorption describing the solute uptake rate, which, in turn, governs the residence time of the sorption reaction, is one of the important characteristics defining the efficiency of sorption.[34] The linear form of the pseudo-first-order rate equation by Lagergren is expressed as Eqn. 5

$$ln(q_e - q_t) = lnq_e - k_1 t \qquad (6)$$

The linear form of the pseudo-second order rate equation is given as,[35]

$$\frac{t}{q_t} = \frac{1}{k_2 q_e^2} + \frac{t}{q_e} \qquad (7)$$

where

q_e and q_t are the amounts of sorbed Th(IV) on magnetic bentonite and sodium bentonite at equilibrium and at time *t*, respectively (mg g^{-1}),
k_1 is the first-order adsorption rate constant (min^{-1}),
k_2 is the pseudo-second-order adsorption rate constant (g mg^{-1} min^{-1}).

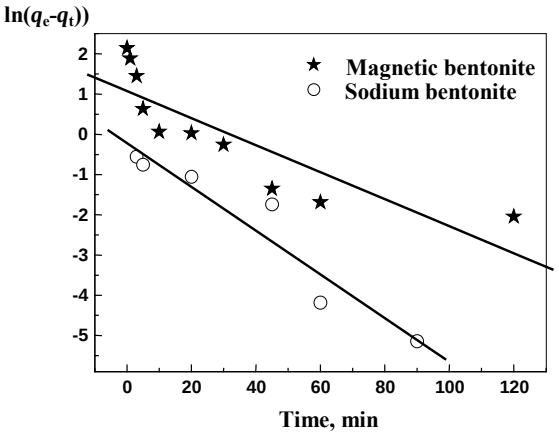

Figure 2. Pseudo-first order plot of Th(IV) adsorption kinetics onto the magnetic and sodium bentonites as a function. *w* = 0.01 g, *V* = 4 mL, Ø = 250 rpm. *T*= room temperature.

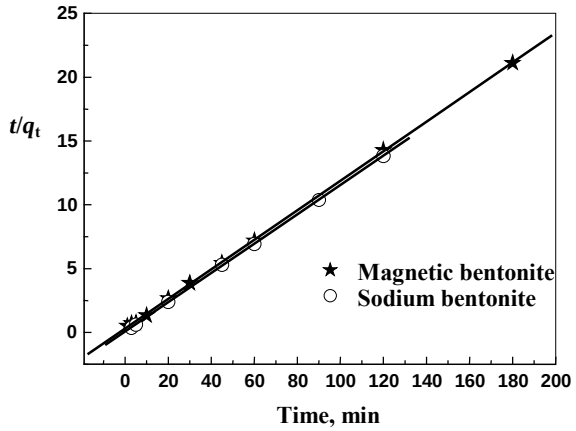

Figure 3. Pseudo-second-order plot of Th(IV) adsorption kinetics onto the magnetic and sodium bentonites as a function. w = 0.01 g, V = 4 mL, Ø = 250 rpm, T= room temperature.

The correlation coefficients (r) for the pseudo-first-order equation and the theoretical q_e values calculated from the pseudo-first-order equation are not in agreement with the experimental data (Table 1), suggesting that this adsorption system is not a pseudo-first-order reaction. High correlation coefficients are obtained when employing the pseudo-second-order model and the calculated equilibrium sorption capacity is similar to the experimental data (Table 1). This indicates that the pseudo-second order model can be applied to predict the adsorption kinetic. Boyd et al. relationship represents an intra-particle diffusion model as follows:[36]

$$\frac{q_t}{q_e} = 1 - \frac{6}{\pi^2} \sum_{n=1}^{ex=1+\frac{x}{1!}+\frac{x^2}{2!}+\frac{x^3}{3!}+\ldots,-\infty<x<\infty} \frac{1}{n^2} \exp\left(-\frac{Dn^2\pi^2}{r^2}t\right) \quad (8)$$

where

D is the intra-particle diffusion coefficient and

r is the particle radius.

For short times (when q_t/q_e is less than 0.3), Eqn. 8 can be reduced to Eqn. 9.

$$q_t = k_{ID}\sqrt{t} \quad (9)$$

where

k_{ID} is the intra-particle diffusion constant.

The significant property of this equation is that, if the intra-particle diffusion is the only rate-limiting step, then the linear plot of q_t versus $t^{1/2}$ should pass through the origin. On the other hand, if the intercept of plots do not equal zero, then it indicates that the intra-particle diffusion is not the sole rate determining step.[37] Then Eqn. 9 is modified to, [38]

$$q_t = k_{ID}\sqrt{t} + S \quad (10)$$

where S is a constant and reflects the boundary layer effect.

Investigation of various reports about the sorption rate shows that the intra-particle diffusion model is the most popular one for the diffusion rate-controlling step that has been used in conjunction with the surface reaction models to recognize the adsorption kinetics.

The plot of the Boyd relationship for the sorption of thorium, at initial concentration equal to 0.1 mmol L^{-1}, by sodium bentonite and magnetic bentonite is shown in Figure 4. Therefore, from Figure 4 it follows that the intra-particle diffusion (at the later portion) proceeds faster than the film diffusion (at the beginning portion). Moreover, the second stage of the lines does not pass through the origin. This means that the intra-particle diffusion, although important over longer contact time periods, is not the rate-limiting step in the adsorption process. The intra-particle diffusion constants and regression coefficients for these two stages (k and R^2) are given in Table 2.

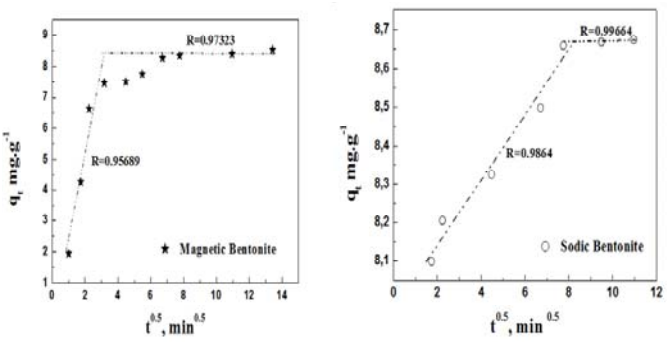

Figure 4: Intra-particle diffusion Kinetic models for the adsorption of Th^{4+}, $[Th(IV)]_0=10^{-4}$ mol L^{-1}, w = 0.01 g, V = 4 mL, Ø = 250 rpm, T= room temperature.

Table 1. Comparison of the pseudo-first order and pseudo-second order models for the adsorption of thorium.

Adsor--bent	q_e (exp.) mg g^{-1}	Pseudo-first order	Pseudo-second order
Sodium bentonite	8.65	r = 0.95904 q_e(calc.)= 0.805 mg g^{-1} K_1=0.05442	r = 0.99997 q_e(calc.)=8.71 mg g^{-1} K_2=0.2109
Magnetic bentonite	8.26	r = 0.86008 q_e(calc.) = 1.076 mg g^{-1} K_1=0,03356	r = 0.99991 q_e(calc.)=8.63 mg g^{-1} K_2=0.0451

Table 2. Intra-particle diffusion model parameters for thorium adsorption onto sodium bentonite and magnetic bentonite

Adsorbent	Intra-particle diffusion model parameters	
	Stage 1	Stage 2
Sodium bentonite	r =0.9864 K= 0.0835 mg g^1 $min^{0.5}$	r =0.99664 K=0.0047 mg.g^{-}.$min^{0.5}$
Magnetic bentonite	r = 0.95689 K= 2.626 mg g^{-1} $min^{0.5}$	r = 0.97323 K= 0.0346 mg g^{-1} $min^{0.5}$

Diffusion study

The thorium(IV) ions transport from the solution phase to the surface of the sodium bentonite and magnetic bentonite particles occurs in several steps viz., the diffusion of ions from the solution to the sodium bentonite and magnetic bentonite surface, the diffusion of ions within the solid extractant, chemical reactions between ions and functional groups of the bentonites.

If the liquid film diffusion controls the rate of exchange, the Eqn. 11 can be used.

$$-ln(1-F) = kt \qquad (11)$$

where

F is the fractional attainment of equilibrium, which is expressed as $F=q_t/q_e$.

If the case of diffusion of ions in the sodium bentonite and magnetic bentonite phase controlling process, the relation used is Eqn.12.

$$-ln(1-F^2) = kt \qquad (12)$$

In both Eqns. 11 and 12, k is the kinetic coefficient or rate constant. k is defined by Eqn. 13.

$$k = \frac{D_r \pi^2}{r_0^2} \qquad (13)$$

where

D_r is the diffusion coefficient in the sodium bentonite and magnetic bentonite phase and

r is the average radius of sodium and magnetic bentonite.

When the adsorption of metal ion involves mass transfer accompanied by chemical reaction the process can be explained by the moving boundary model. This model assumes a sharp boundary that separates a completely reacted shell from an unreacted core and that advances from the surface toward the center of the solid with the progression of adsorption. In this case, the rate equation is given by Eqn. 14.[34, 35]

$$3 - 3(1-F)^{2/3} - 2F = kt \qquad (14)$$

Testing both mathematical models proposed above (Figure 5), indicates that film diffusion model is adequate for magnetic bentonite, however, adsorption can be explained by both the diffusion models for sodium bentonite.

Table 3. Kinetic and diffusion parameters of thorium onto magnetic bentonite and sodium bentonite.

Adsorbent	Film diffusion Eqn. 6	Particle diffusion, Eqn. 7	Chemical reaction, Eqn. 8
Sodium bentonite	K= 0.0544 min^{-1} R = 0.95904	K= 0.0540 min^{-1} R = 0.95852	K = 0.0041 min^{-1} R = 0.96773
Magnetic bentonite	K = 0.0415 min^{-1} R = 0.97369	K = 0.0057 min^{-1} R = 0.93072	K = 0.00805 min^{-1} R = 0.96492

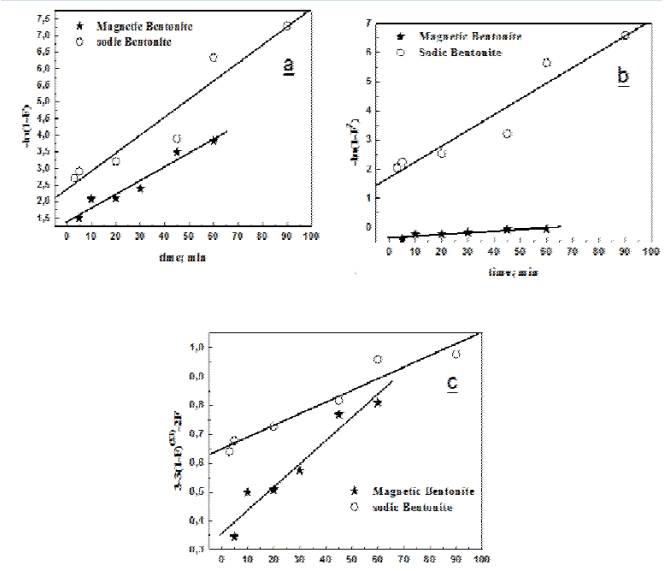

Figure 5. Plots of diffusion study for Th(IV) sorption on Magnetic bentonite and sodium bentonite at different time. $[Th(IV)]_0=10^{-4}$ mol L^{-1}, w = 0.01 g, V = 4 mL, Ø = 250 rpm, T= room temperature: Film diffusion (a), internal diffusion (b), chemical reaction (c).

Effect of pH

Sorption of thorium by magnetic bentonite and sodium bentonite were studied at different pH ranging from 1.43 to 9.35 and the results are show in Figure 6. The extraction yield, with magnetic bentonite is very low acidic region and the removal of thorium begins to increase with increase in pH and reaches a maximum value in the pH 6.20, decreasing at higher pH. In pH in the range of 1.4-5.1, hydrogen ions compete strongly with Th(IV) ions for the active sites, which results in less metal sorption. As the hydrogen ion concentration dcreases, thorium(IV) ions sorption increases. At pH is 6.2, a large number of active adsorption sites are released, so there are the maximum Th(IV) sorption efficiency at the pH values 6.2. Beyond pH 6.2, insoluble thorium hydroxide started precipitating, which leads to low Th(IV) ions sorption efficiency.[10] The variation initial pH has no influence on the extraction yield for sodium bentonite, which is between 80 % and 85 %.

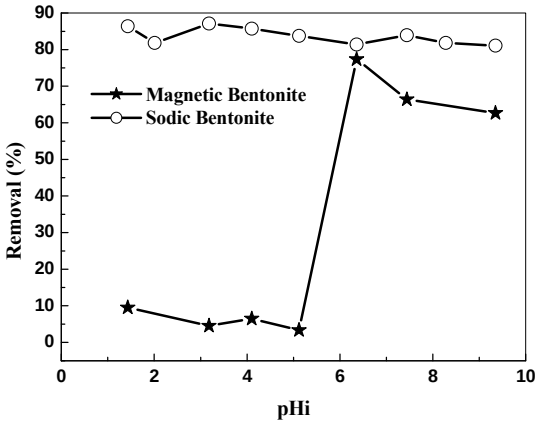

Figure 6. Removal of thorium by magnetic and sodium bentonites as a function of initial pH.

Effect of initial metal concentration

Several experiments were also undertaken to study the effect of varying the initial thorium concentration on uptake (q) from the solution by 0.01 g of the adsorbent. The amount of Th(IV) sorbed per unit mass of the particles magnetic increased with the initial metal concentration.

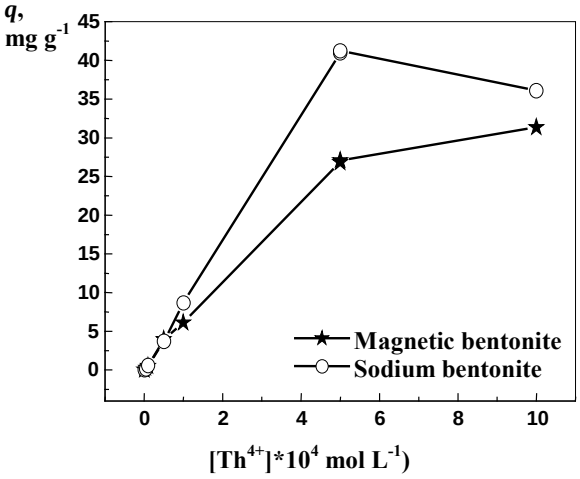

Figure 7. Removal of thorium by magnetic and sodium bentonites as a function of [Th(IV)]. w = 0.01 g, V = 4 mL, Ø = 250 rpm, T= room temperature.

Figure 7 show that the maximum sorption capacities for the metal ions were 41.24 mg.g^{-1} (0.177 mmol g^{-1}) for sodium bentonite and 31.34 mg.g^{-1} (0.135 mmol g^{-1}) for magnetic bentonite, this values indicate that sodium bentonite and magnetic bentonite were effectives sorbents in treatment of diluted thorium solutions. This sorption capacity is comparatively higher than those of some other sorbent materials reported in the literature (Table 4).

Isotherm adsorption

The sorption data, commonly known as adsorption isotherms, are basic requirements for the design of adsorption systems. Classical adsorption models, Langmuir (Eqn.15) and Freundlich (Eqn. 16), were used to describe the equilibrium between adsorbed Th(IV) ions on the sodium and magnetic bentonite site.[35] For the interpretation of both models, we have used the following equations.[47]

$$\frac{C_e}{q_e} = \frac{C_e}{q_m} + \frac{1}{q_m K_L} \quad (15)$$

$$\ln q_e = \ln K_F + n \ln C_e \quad (16)$$

where

C_e is the equilibrium concentration of thorium (mg L^{-1}),

q_e is the amount of thorium sorbed on the sodium and magnetic bentonite (mg g^{-1}),

k_L is the Langmuir adsorption constant (L mg),

q_{max} is the maximum amount of thorium that can be sorbed,

k_F is the Freundlich adsorption constant and

n is a constant that indicates the capacity and intensity of the adsorption, respectively.

Table 4. The comparison of adsorption capacity of sodium and magnetic bentonite for thorium with those of various other sorbents reported in the literature.

Adsorbent	Sorption capacity (mmol g^{-1})	Reference
Activated carbon	0.087	18
PAN/zeolite	0.04	22
Resin (MCM)	0.984	39
Amberlite XAD-4	0.25	20
SiO_2	0.001	40
MX-80	0.275	42
Amberlite XAD	0.113	43
Perlite	0.025	44
Modified clay MTTZ	0.116	19
Attapulgite	0.067	45
Raw diatomite	0.03	46
Calcined diatomite	0.06	7
Flux calcined diatomite	0.05	7
Sodium bentonite	0.177	This work
Magnetic bentonite	0.135	This work

Under the given reaction conditions, experimental data correlate better with Langmuir isotherm (Fig. 8) than with Freundlich isotherm (Fig. 9). From adsorption equilibrium of thorium ions by magnetic bentonite and sodium bentonite, a monolayer adsorption is suggested. The maximum adsorption values were in accordance with the values obtained experimentally (Table 5).

Effect of ionic strength

The effect of $NaNO_3$, CH_3COONa, $Na_2S_2O_3$ on the performance of extraction was studied. Figures 10 and 11 show that the influence of the ionic strength on sorption of thorium is important.

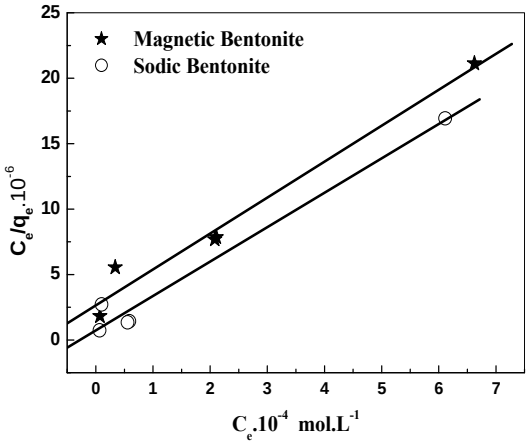

Figure 8. Langmuir isotherm plot for the sorption of Th(IV) onto sodium and magnetic bentonite.

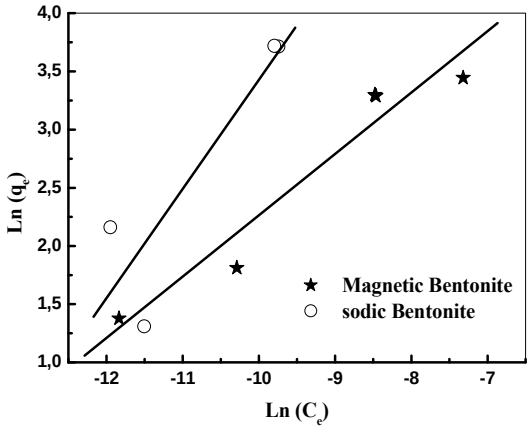

Figure 9. Freundlich isotherm plot for the sorption of Th(IV) onto sodium and magnetic bentonite.

Table 5. Isotherm models parameters for the adsorption of Th(IV) on magnetic bentonite and sodium bentonite

Adsorbent	q_m(exp.)	Langmuir isotherm	Freundlich isotherm
Sodium bentonite	41.24 mg g^{-1}	r = 0.9883 q_m(calc.) = 38.03 mg g^{-1} K_L = 9927.7	r = 0.8983 K_F = 362217.44 n = 0.9380
Magnetic bentonite	31.34 mg g^{-1}	r = 0.9863 q_m(calc.) =36.44 mg g^{-1} K_L=10362.69	r = 0.9663 K_F = 1881.83 n=0.527

Changing the ionic strength by the addition of an electrolyte influences adsorption in at least two ways ,[48,49] one by affecting interfacial potential and therefore the activity of electrolyte ions and adsorption and secondly by affecting the competition of the electrolyte ions and adsorbing anions for sorption sites.

It is evident in Figure 10 , that there is a positive impact on increasing $Na_2S_2O_3$ concentration from 0.077 M to 0.123 M (100% of removal), the addition of $NaNO_3$ in a concentration less than 0.7 M decreased extraction yield of Th(IV), this can be explained by a competitiveness in the extraction between Th^{4+} and Na^+,[50] but at concentrations [$NaNO_3$] ≥ 0.7 M extraction efficiency increased to 100 % at 0.8 M, , it may due to the common ion effect that lowers the solubility of Th(IV) salt.[51] From 0.1M to 1M, the effect of CH_3COONa is negligible.

Figure 11 show that the extraction yield of Th(IV) increases with the increasing of the $Na_2S_2O_3$ concentration from 0.042 M until it reaches its maximum value of 100% at 0.077 M. The addition of CH_3COOH decreased extraction yield of Th(IV), this effect is attributed to the competition between Na^+ provided by the addition of salt and Th(IV) in the formation of bonds with the active sites of sodium bentonite. The addition of $NaNO_3$ has no influence on the extraction of Th(IV).

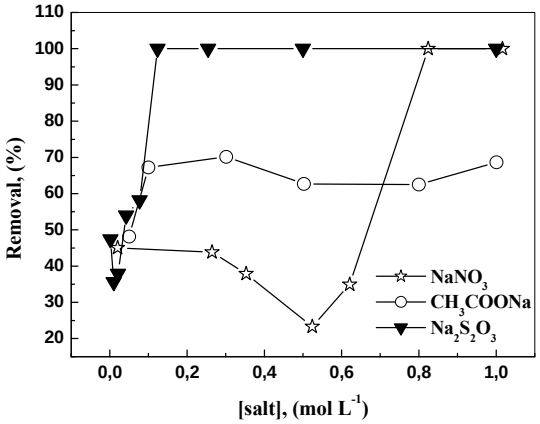

Figure 10. Removal of thorium by magnetic bentonites as a function of electrolytes under standard conditions.

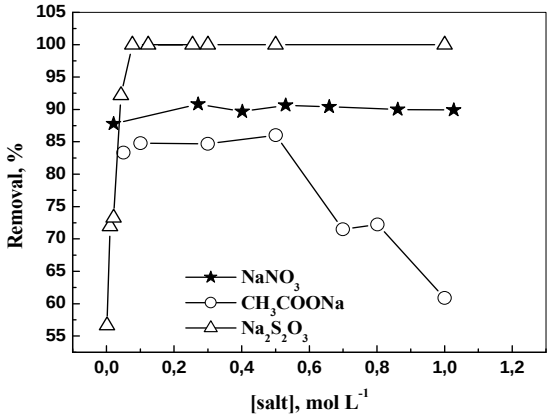

Figure 11. Removal of thorium by sodium bentonite as a function of electrolytes under standard conditions.

TG Analysis and DSC of the modified bentonite

The amount of intercalated product deduced from the TGA experiment for magnetic bentonite was shown in Figure 12.

Concerning the dried sodium bentonite pattern, 1.128 % weight-loss was checked at the temperature range of 59.61-123.15 °C, 1.982 % weight-loss appeared at 472.48–591.97 °C and 1.708 % weight-increase appeared at 873.61-880.48 due to the absorption of the nitrogen.

Concerning the dried bentonite magnetic pattern, 6.362 % weight-loss was checked at the temperature range of 39.00-121.43 °C, 1.187 % weight-loss appeared at 171.24-231.34 °C, 1.077 % weight-loss appeared at 301.82-396.74 °C and 1.50 % weight-loss appeared at 567.71-664.01 °C. The low values of weight-loss show a good thermal stability for sodium bentonite and magnetic bentonite.

The difference between the weight-loss of the sodium bentonite and the magnetic bentonite can be explained by the quantity of magnetic particles grafted into the sodium bentonite which corresponds to 8.4 %.

The TGA curve of bentonite shows two marked departures of water, one at low temperature (less than 110°C) corresponding to the hygroscopic water, the second at 470-540 °C corresponding to the loss of structural water. According to literature data,[52] we can attribute the different mass losses for different types of interactions between the water and bentonite. Below 80 °C, adsorbed water is lost. Between 80 and 110 °C, chemisorbed water in the porous structure of bentonite is lost. Water formed from the recombination of the OH groups of the structure is lost between 470 and 540 °C.

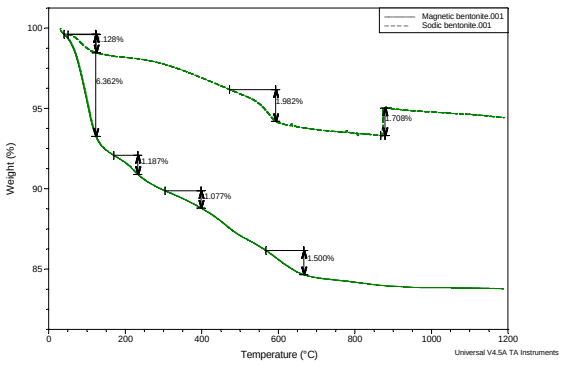

Figure 12. TGA patterns of sodium bentonite and magnetic bentonite.

The comparison between the DSC of the sodium bentonite and the magnetic bentonite (Figure 13) shows that the transition of phases were not any more the same. This is due to the presence of the maghemite in the structure of the bentonite.

Thermodynamic Parameters

The effect of temperature on the sorption of thorium from nitrate solution by sodium bentonite and magnetic benonite at pH 6.2, *V*=4 mL, *w*=0.010 g, Ø=250 rpm and concentration Th(IV) 10^{-4} mol L^{-1} was studied for the determination of thermodynamic data such as, the Gibbs free energy change (ΔG), enthalpy change (ΔH) and entropy change (ΔS). ΔG was calculated using the following equations :[53]

$$\Delta G = \Delta H - T\Delta S \qquad (17)$$

$$\Delta G = -RT \ln D \qquad (18)$$

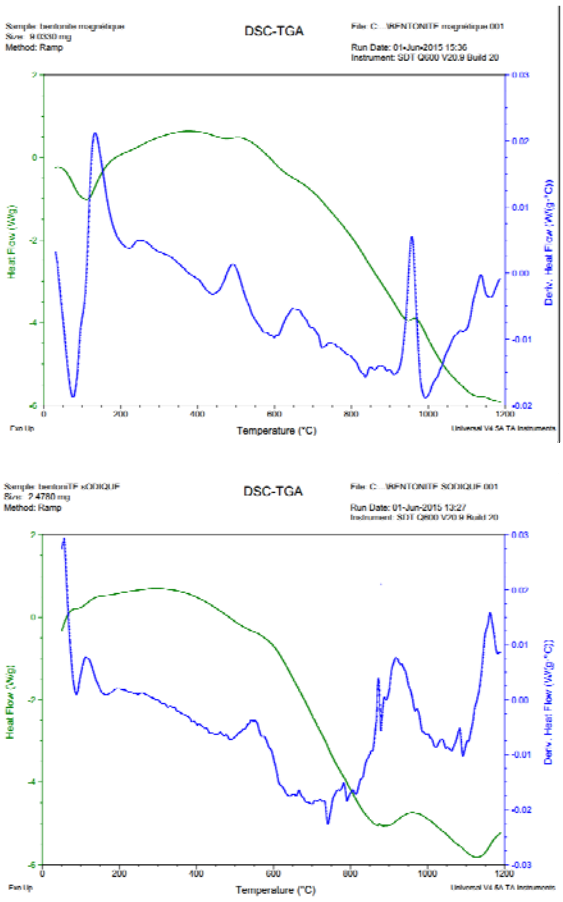

Figure 13. Differential scanning calorimetry of magnetic bentonite and sodium bentonite

where

R is the gas constant (8.314 J $mol^{-1}K^{-1}$), and

T the temperature (K).

The relation between D, ΔH and ΔS can be described by Van't Hoff correlation in Eq.19.[54]

$$\ln D = \frac{\Delta S}{R} - \frac{\Delta H}{RT} \qquad (19)$$

Figure 14 shows removal percent (%) of thorium ion onto sodium bentonite and magnetic bentonite as a function of the temperature. It can be seen that the yield extraction of Th(IV) increases with increasing temperature for magnetic bentonite, this behaviour indicates that thorium sorption onto magnetic bentonite is an endothermic and spontaneous process, as supported by the positive values of ΔH and ΔS (Fig. 15 and Table 6); decrease in ΔG values with increase in temperature showed that the sorption was most favourable at higher temperature.

In contrast, increasing temperature from 25 °C to 50 °C was found to have a detrimental effect on the extraction process for sodium bentonite, the negative value of ΔH indicate that the extraction process is exothermal.[50, 35]

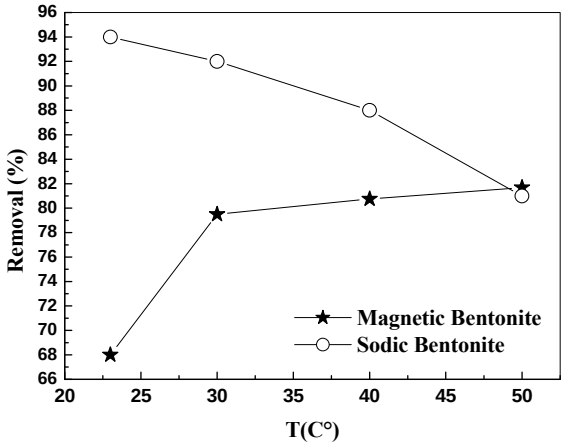

Figure 14. Removal of thorium by magnetic and sodium bentonites as a function of temperature. $[Th(IV)]_0=10^{-4}$ mol L^{-1}, *w* = 0.01 g, *V* = 4 mL, Ø = 250 rpm.

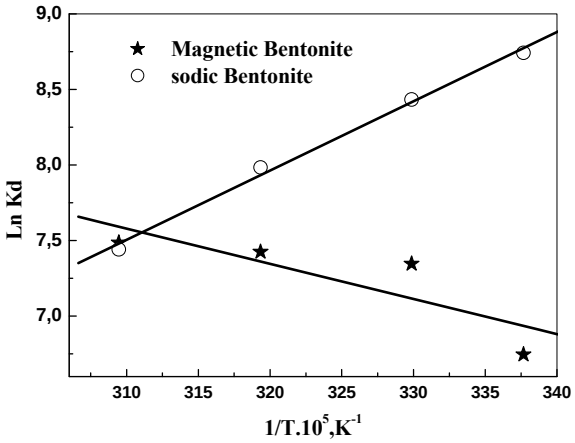

Figure 15. Plot of Eq.6 for the thorium sorption on by magnetic and sodium bentonites.

Table 6. Thermodynamic parameters for the sorption of Th(IV) on sodium and magnetic bentonite.

Material	ΔH (kJ mol^{-1})	ΔS (J mol^{-1} K^{-1})	ΔG(kJ mol^{-1}) at 303 K
Sodium bentonite	-38.1	-55. 8	-21.2
Magnetic bentonite	5.7	79.9	-18.52

Desorption Study

In order to investigate the elution behavior of Th(IV) from the sodium bentonite and magnetic bentonite, elution experiments were conducted with using various eluting agents viz, CH_3COOH, H_2SO_4, HNO_3, and HCl of a concentration of 0.5 mol L^{-1}. Firstly, sodium bentonite and magnetic bentonite are saturated with the solution of thorium and elution yield is calculated by Eqn. 5. To a saturated sample the appropriate bentonite (0.01 g), 4 mL of the selected acid was added and kept for 3 h. Though all the acids gave significant elution yield for sodium bentonite, for magnetic bentonite better yields was obtained with CH_3COOH (78 %) and H_2SO_4 (100 %).

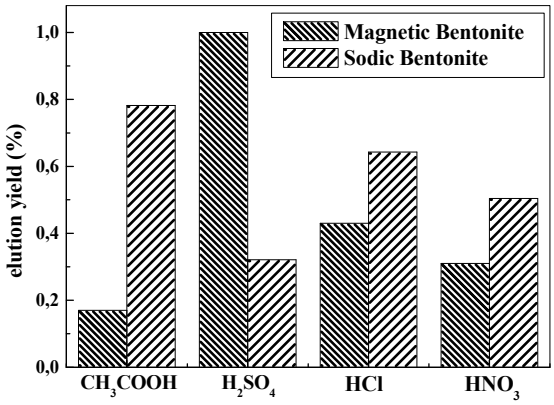

Figure 16. Optimum eluants for quantitative recovery of thorium.

Conclusion

In this investigation, liquid-solid extraction of Th(IV) is made with sodium bentonite and magnetic bentonite. The extraction efficiency was determined as a function of various parameters such as time, initial pH, Thorium concentration, temperature and ionic strength. The experimental capacity obtained was 31.34 mg g^{-1} for magnetic bentonite and 41.24 mg g^{-1} for sodium bentonite. The sorption of Th(IV) achieves equilibration at 45 minutes and 60 minutes for magnetic bentonite and sodium bentonite, respectively. Optimal extraction yield was achieved in a initial pH equal at 6.2 for magnetic bentonite, By against, the variation of initial pH has no influence on the extraction yield. Desorption study of thorium can be effected with acetic acid 0.5 mol L^{-1} and sulfuric acid 0.5 mol L^{-1} for sodium bentonite and magnetic bentonite, respectively after 3 h of shaking.

There is not much difference between the bentonites, but magnetic bentonite have a unique superiority in separation, it can be quickly separated from a medium by a simple magnetic process. In view of the results obtained in this study, magnetic bentonite can be a promising material for sorption, immobilization and pre-concentration of rare earth elements, radioactive metal and heavy metal ions from large volume of solutions.

References

[1]Guerraa, D., Vianab, R., Airoldi, C., *J. Hazard. Mater.,* **2009**, *168*, 1504-1511.

[2]Rahmani-Sani, A., Hosseini-Bandegharaeia, A., Hosseinib, S., Kharghani, K., Zarei, H., Rastegar, A., *J. Hazard. Mater*., **2015**, *286*, 152-163.

[3]Phillips, D. H., Watson, D. B., *J. Hazard. Mater.,* **2015**, *285*, 474-482.

[4]Hritcua, D., Humelnicub, D., Dodia, G., Popa, M., *Carbohyd. Polym.*, **2012**, *87*, 1185-1191.

[5]Anirudhan, T. S., Sreekumari, S. S., Jalajamony, S., *J. Environ. Radioactiv.,* **2013**, *116*, 141-147.

[6]Huang, H., Ding, S., Su, D., Liu, N., Wang, J., Tan, M., Fei, J., *Sep. Purif. Technol*., **2014**, *138*, 65-70.

[7]Yusan, S., Gok, C., Erenturk, S., Aytas, S., *Appl. Clay Sci.,* **2012**, *67–68*, 106-116.

[8]Anirudhan,T. S., Jalajamony, S., *J. Environ. Sci*., **2013**, *25(4)*, 717-725.

[9]Khajeha, M., Pedersen-Bjergaard, S., Barkhordar, A., Bohlooli, M., *Spectrochim. Acta A*, **2015**, *137*, 328-332.

[10]Yang, S. K., Tan, N., Yan, X, M., Chen, F., Long, W., Lin, Y, C., *Mar. Pollut. Bull*., **2013**, *74*, 213-219.

[11]Nilchi, A., Shariati Dehaghan, T., Rasouli Garmarodi, S., *Desalination*, **2013**, *321*, 67-71.

[12]Chandramouleeswaran, S., Ramkumar, J., *J. Hazard. Mater.*, **2014**, *280*, 514-523.

[13]Metaxasa, M., Kasselouri-Rigopoulou,V., Galiatsatou, P., Konstantopoulou, C., Oikonomou, D., *J. Hazard. Mater. B97*, **2003**, 71-82.

[14]Akkaya, R., *J. Environ. Radioactiv.,* **2013**, *120*, 58-63.

[15]Anirudhan, T., Rijith, S., Tharun, A., *Colloid. Surface A*, **2010**, *368*, 13-22.

[16]Abbasizadeh, S., Reza Keshtkar, A., Mousavian, M., *Chem. Eng. J.*, **2013**, *220*, 161-171.

[17] Bradbury, M. H., Baeyens, B., *Geochim. Cosmochim. Ac.*, **2005**, *69 (4)*, 875-892.

[18]Kütahyalı, C., Eral, M., *J. Nucl. Mater.*, **2010**, *396*, 251-256.

[19]Guerraa, D., Viana, R., Airoldi, C., *J. Hazard. Mater.*, **2009**, *168*, 1504-1511.

[20]Dev, K., Pathak, R., Rao, G., *Talanta*, **1999**, *48*, 579-584.

[21]Murphy, R., Lenhart, J., Honeyman, B., *Colloid. Surface A*, **1999**, *157*, 47-62.

[22]Kilincarslan Kaygun, A., Akyil, S., *J. Hazard. Mater.*, **2007**, *147*, 357-362.

[23]Makhoukhi, B., Djab, M., Didi, M. A., *J. Environ. Chem. Eng.*, **2015**, 3, 1384-1389.

[24]Bulut, Y., Akçay, G., Elma, D., Ersin Serhatli, I., *J. Hazard. Mater.*, 2009, *171*, 717-723.

[25]Wu, L., Ye, Y., Liu, F., Tan, C., Liu, H., Wang, S., Wang, J., Yi, W., Wu, W., *Appl. Clay Sci.*, **2013**, *83–84*, 405-414.

[26]Makhoukhi, B., Didi, M. A., Moulessehoul, H., Azzouz, A., Villemin, D., *Appl. Clay Sci.*, **2010**, *50*, 354-361.

[27]Chen, Y., Zhu, B., Wuc, D., Wangc, Q., Yang, Y., Ye, W., Guo, J., *Chem. Eng. J.,* **2012**, *181–182*, 387-396.

[28]Lian, L., Cao, X., Wua, Y., Sun, D., Lou, D., *Appl. Surf. Sci.,* **2014**, *289*, 245-251.

[29]Idris, A., Ismail, N., Hassan, N., Misran, E., Ngomsik,A., *J. Ind. Eng. Chem.,* **2012**, *18*, 1582-1589.

[30]Miraoui, A., Didi, M. A., Villemin. D., *J. Radioanal. Nucl. Chem*., **2015**, doi : 10.1007/s10967-015-4267-2. In press.

[31]Panneerselvam, P., Morad, N., Lim, Y., *Sep. Sci. Technol.,* **2013**, *48*, 2670-2680.

[32]Sapag, K., Rios, R. V. R. A., Fabris, J. D., Oliveira, L. C. A., Lago, R. M., *J. Chem. Edu.,* **2004**, *81*, 248-250.

[33]Bayyaria, M. A., Nazal, M .K., Khalili, F, A., *J. Saudi Chem. Society*, **2010**, *14*, 311-315.

[34]Benaissa , E., Abderrahim, O., Didi , M. A., *J. Radioanal. Nucl. Chem*. **2014**, *299*, 439-446.

[35]Ferrah, N., Abderrahim, O., Didi, M. A., Villemin, D., *J. Radioanal. Nucl. Chem*., 2011, *289*, 721-730.

[36]Boyd, G. E., Adamson, A.W., Jr Myers, L, S., *J. Am. Chem. Soc.,* **1947**, *69*, 2836-2848.

[37]Haerifar, M., Azizian, S., *J. Phys. Chem. C*., **2013**, *117*, 8310-8317.

[38]Barkakati, P., Begum, A., Das, M, L., *Chem. Eng. J*., **2010**, *161*, 34-45.

[39]Ferrah, N., Abderrahim, O., Didi, M. A., Villemin, D., *Desalination*, **2011**, *269*, 17-24.

[40]Raju, Ch. S. K., Subramanian, M. S., *J. Hazard. Mater.*, **2007**, *145*, 315-322.

[41]Chen, C., Wang, X., *Appl. Radiat. Isotopes,* **2007**, *65*, 155-163.

[42]Zhao, D. L., Feng, S. J., Chen, C. L., Chen, S. H., Xu, D., Wang, X. K., *Appl. Clay Sci.*, **2008**, *41*, 17-23.

[43]Seyhan, S., Merdivan, M., Demirel, N., *J. Hazard. Mater.*, **2008**, *152*, 79-84.

[44]Talip, Z., Eral, M., Hicsonmez, U., *J. Environ. Radioactivity,* **2009**, *100*, 139-143.

[45]Chen, L., Gao, X., *Appl. Radiat. Isotopes*, **2009**, *67*, 1-6.

[46]Sheng, G., Hu, J., Wang, X., *Appl. Radiat. Isotopes*, **2008**, *66*, 1313-1320.

[47]Kul, A. R., Koyuncu, H., *J. Hazard. Mater.*, **2010**, *179*, 332-339.

[48]Abderrahim, O., Didi, M. A., Villemin, D., *J. Radioanal. Nucl. Chem*., **2009**, *279 (1)*, 237-244.

[49]Vilar, V. J. P., Botelho C. M. S, Boaventura, R.A.R., *Process Biochem*., **2005**, *40*, 3267-3275.

[50]Didi, M. A., Villemin, D., Abderrahim, O., Azzouz, A., *J. Radioanal. Nucl. Chem.*, **2014**, *299*, 1191-1198.

[51]Abderrahim, O., Didi, M. A., Villemin, D., *Anal. Lett.*, **2009**, *42***,** 1233-1244.

[52]Keller L., Thesis of chemistry. **2004**, Haute Alsace University, p.198.

[53]Kadous, A., Didi, M. A., Villemin, D., *J. Radioanal. Nucl. Chem.*, **2010**, *284*, 431-438.

[54]Zhao, Y., Liu, C., Feng, M., Chen, Z., Li, S., Tian, G., Wang, L., Huang, J., Li, S., *J. Hazard. Mater.,* **2010**, *176(1–3)*, 119-124.

Received: 05.11.2015.
Accepted: 08.12.2015.